Equivalent Circuit Modeling of DC and AC Ferrite Magnetic Properties Using H-input and B-input Play Models

S. Ito[1], T. Mifune[1], T. Matsuo[1], *Member IEEE*,
K. Watanabe[2], H. Igarashi[3], K. Kawano[4], Y. Iijima[5], M. Suzuki[4], Y. Uehara[6], A. Furuya[6]
[1]Graduate School of Engineering, Kyoto University, Kyoto, 615-8510, JAPAN
[2]Muroran Institute of Technology, [3]Hokkaido University, [4]Taiyo Yuden Co., Ltd.,
[5]Oyama National College of Technology, [6]Fujitsu Ltd.

An equivalent circuit model is proposed to represent ferrite magnetic properties under AC and DC fields phenomenologically, where H-input and B-input play models are used to handle hysteretic property accurately and concisely. A slow magnetization component is extracted from measured AC and DC properties. Frequency dependence of the AC loss is represented by an equivalent resistance. The simulated AC and DC magnetic properties agree with the measured properties.

***Index Terms*—AC property, equivalent circuit, ferrite, play model.**

I. Introduction

Ferrite [1] is widely used as a core material for high frequency use. For example, electric power circuits such as a DC-DC converter often have ferrite cored reactors, where the AC ferrite property needs to be evaluated under a DC biased field. However, its simulation is not easy because a minor hysteresis loop representation under the DC biased field is required. Accordingly, an accurate hysteresis model is required to describe both the AC and DC magnetic properties of a ferrite core.

Complex hysteresis properties including minor loops can be described by several hysteresis models such as the Preisach model [2], [3] the play model [4]-[7] and the stop model [4], [6], [8]. The play model is a simple and accurate hysteresis model which property is equivalent to the classical Preisach model [5]. It is a convenient tool for processing hysteretic data because it can efficiently describe both hysteretic functions providing the output of the magnetic flux density B from the input of magnetic field H and the output H from the input B. However, the play model requires an additional dynamic term [9] to represent the rate-dependent hysteretic property because the play model is basically a static model.

This paper develops a phenomenological modeling method to derive an equivalent circuit from measured AC and DC hysteretic properties, where the H-input and B-input play models are used to handle the hysteretic property accurately and concisely.

II. Equivalent Circuit Representation

NiZn ferrite has high resistivity of ~10^7 Ω·m in general and yields little eddy-current field. Accordingly, the AC core loss consists of hysteresis loss and residual loss [11]. It has been said that the latter is mostly due to a domain wall damping. However, its origin has not been made clear in detail. This study develops a phenomenological model of rate-dependent property of NiZn ferrite.

Manuscript received November 8, 2012 (date on which paper was submitted for review). Corresponding author: T. Matsuo (e-mail: tmatsuo@kuee.kyoto-u.ac.jp).
Digital Object Identifier inserted by IEEE

DC and AC magnetic properties of a NiZn ferrite ring core are measured. The magnetic field H is obtained from the excitation current of the primary winding and the magnetic flux density B is given by the integration of voltage of the secondary winding. Since the DC component of B cannot be measured directly, the DC magnetic property is obtained from measurements at very low frequency.

Fig. 1(a) shows hysteretic properties of ferrite ring core under the condition of a sinusoidal magnetic flux density at 100-800 kHz. Fig. 2 plots the relationship between the coercive force H_C and ωB_a, where B_a is the amplitude of B and ω is the angular frequency. The coercive force increases in proportion to ωB_a. Accordingly, this AC magnetic field H_{AC} is approximated in this study as

$$H_{AC}(B) = h_{fast}(B) + (1/R_1)\, dB/dt \qquad (2)$$

where $h_{fast}(B)$ represents the rate-independent hysteretic property and R_1 is a constant. After R_1 is determined from the frequency dependence of coercive force as in Fig. 2, $h_{fast}(B)$ is obtained by $H_{AC}(B) - (1/R_1)\, dB/dt$.

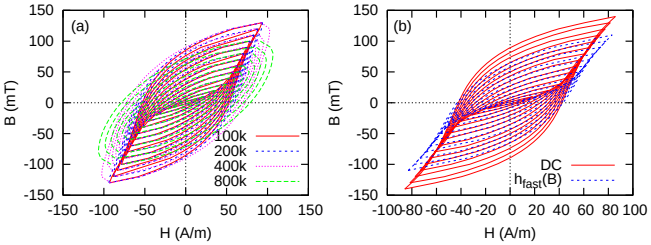

Fig. 1 Measured BH loops: (a) at 100-800 kHz, and (b) at DC.

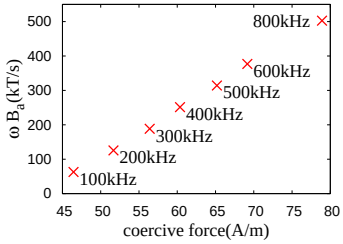

Fig. 2 Relationship between the coercive force and ωB_a with B_a = 100mT.

Fig. 1(b) plots measured DC property, where the DC magnetic field yields a higher B compared with $h_{\mathrm{fast}}(B)$. Accordingly, this paper assumes that the DC magnetization process is decomposed into fast and slow components as

$$B_{\mathrm{DC}} = b_{\mathrm{slow}}(H) + b_{\mathrm{fast}}(H) \tag{1}$$

where the fast component $b_{\mathrm{fast}}(H)$ is represented by the inverse function of $h_{\mathrm{fast}}(B)$ and the slow component $b_{\mathrm{slow}}(H)$ does not respond to the high frequency field.

Nonlinear electric circuit simulations usually use magnetic fluxes as state variables. Assuming the correspondence of B to the magnetic flux ϕ and H to the current I, AC and DC properties, given by (1) and (2), are represented phenomenologically by the equivalent circuit shown in Fig. 3. The circuit equations are given by:

$$\begin{aligned} &I = I_0 + V_0/R_0 + I_{C0} = I_1 + V_1/R_1 + I_{C1} \\ &V_0 = \mathrm{d}\phi_0/\mathrm{d}t, \qquad V_1 = \mathrm{d}\phi_1/\mathrm{d}t \\ &I_{C0} = C_0\,\mathrm{d}V_0/\mathrm{d}t, \quad I_{C1} = C_1\,\mathrm{d}V_1/\mathrm{d}t \\ &I_0 = h_{\mathrm{slow}}(\phi_0), \qquad I_1 = h_{\mathrm{fast}}(\phi_1) \end{aligned} \tag{3}$$

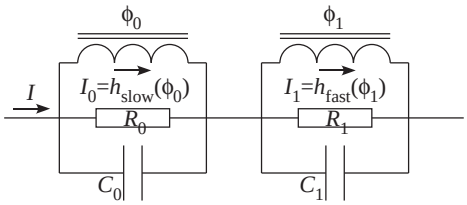

Fig. 3 Equivalent circuit model where I corresponds to H and $\phi_0+\phi_1$ corresponds to B.

The resonance frequency f_0 of the left LCR circuit is lower than that of the right circuit. The left inductor represents the slow component where h_{slow} is the inverse function of b_{slow} and it does not work for frequencies higher than f_0. It is assumed that the right LCR circuit represents a domain-wall resonance.

The hysteretic properties h_{slow} and h_{fast} in the circuit model are represented by the B-input play model whereas the H-input play model is used in the decomposition into slow and fast components. A brief explanation of the play model is given in the Appendix.

The flow of data processing is illustrated in Fig. 4. First, R_1 is determined from the measured AC data with a sinusoidal magnetic flux density. Since the measurement requires the control of B, the B-input play model is conveniently identified from the measured AC data. After extracting $(1/R_1)\mathrm{d}B/\mathrm{d}t$ ([a1] in Fig. 4), the B-input play model is identified to represent the fast component as $H = h_{\mathrm{fast}}(B)$ ([A2]). The inverse relationship $B = b_{\mathrm{fast}}(H)$ is represented by the H-input play model ([A3]). The H-input play model is identified from the symmetric BH loops with the amplitudes of $H_a = nH_S/N_p$ (n = 1, …, N_p), where H_S is the saturation magnetic field and N_p is the number of play hysterons. When the waveform of H with amplitude H_a is given, the corresponding B-waveform is obtained by solving the nonlinear equation for B as:

$$F(B) = H - h_{\mathrm{fast}}(B) = 0\,. \tag{4}$$

Equation (4) is solved using the Newton-Raphson method [10] to identify the H-input play model ([a2]). The slow component $b_{\mathrm{slow}}(H) = B_{\mathrm{DC}}(H) - b_{\mathrm{fast}}(H)$ is also represented by the H-input play model ([B3]). The B-input play model represents the inverted relationship $h_{\mathrm{slow}}(B)$ ([B4]), which is obtained in a similar way to the inversion procedure above.

III. SIMULATION OF DC AND AC PROPERTIES

From the relationship in Fig. 2, R_1 is given as 1.25×10^4 Ω/m. Fig. 5 portrays the BH-loops of the fast component that is given by $H - R_1\,\mathrm{d}B/\mathrm{d}t$ at 100 kHz.

Fig. 6 shows $b_{\mathrm{slow}}(H)$ that is given by $B_{\mathrm{DC}}(H) - b_{\mathrm{fast}}(H)$ ([b2]), where BH curves have been smoothed for the Newton-Raphson procedure ([b3]).

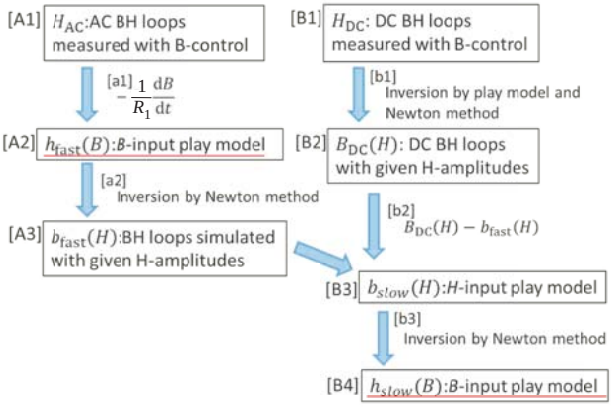

Fig. 4 Flow of data processing.

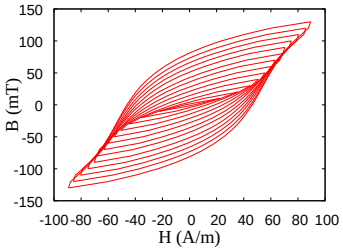

Fig. 5 Fast component.

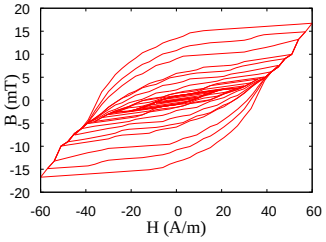

Fig. 6 Slow component.

This study does not focus on the physical origin of slow component. The circuit parameters for the slow component are $C_0 = 8\times10^{-7}$ F·m and $R_0 = 20$ Ω/m so as for the resonance frequency f_0 to be sufficiently lower than the operation frequency around 1 MHz. The parameter C_1 is 7×10^{-14} F·m, which is determined so as for the domain-wall resonance frequency to be higher than 10 MHz.

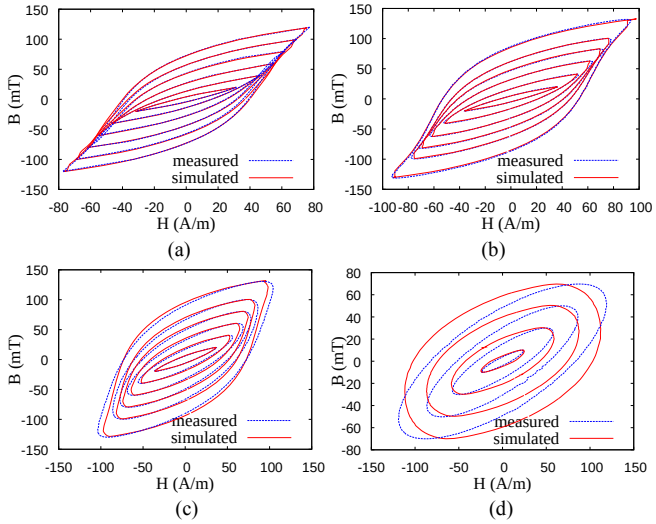

Fig. 7 Simulated BH loops: (a) at DC, (b) at 100 kHz, (c) at 400 kHz, and (d) at 2 MHz.

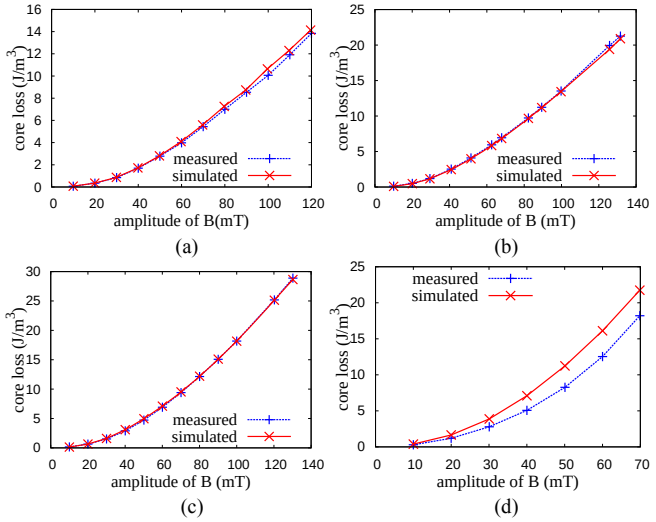

Fig. 8 Core loss per cycle: (a) at DC, (b) at 100 kHz, (c) at 400 kHz, and (d) at 2 MHz.

Fig. 7 portrays simulated DC and AC BH-loops of the ferrite ring core represented by the circuit equation (3). Fig. 8 compares measured and simulated core loss per cycle that is given by the BH-loop area. When frequency is below 400 kHz, the DC and AC properties are accurately reconstructed by the proposed model, where the average evaluation error of the core loss is about 1.7 % at 100 kHz and 0.5 % at 400 kHz.

However, the rate-dependent component is over-estimated at 2 MHz. The discrepancy in the BH loops at 2 MHz is because the circuit parameters are determined below the frequency of 400 kHz. The BH loops in Fig. 7(d) show that the rate-dependent component is not proportional to dB/dt and has a phase lag relative to dB/dt. This study phenomenologically represents the AC property above using the first-order lag element. Accordingly, the equivalent circuit for the fast component is modified as in Fig. 9. The circuit equations for the fast component are replaced by:

$$I = I_1 + I_{R1} + I_{C1}$$

$$V_1 = \mathrm{d}\phi_1/\mathrm{d}t = R_1 I_{R1} + L\mathrm{d}I_{R1}/\mathrm{d}t$$
$$I_{C1} = C_1\, \mathrm{d}V_1/\mathrm{d}t\ ,\ \ I_1 = h_{\mathrm{fast}}(\phi_1)\ . \qquad (7)$$

The parameter L is set to 6×10^{-4} H/m by a parameter fitting.

Fig. 10 portrays the BH loops given by the modified model. The modified model improves the representation accuracy at 2 MHz with a small influence on the simulated properties at low frequency. Fig. 11 shows the core loss per cycle given by the modified model, where the average discrepancies are 1.1 % at 400 kHz and 4.6 % at 2 MHz.

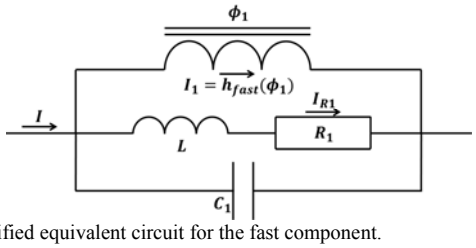

Fig. 9 Modified equivalent circuit for the fast component.

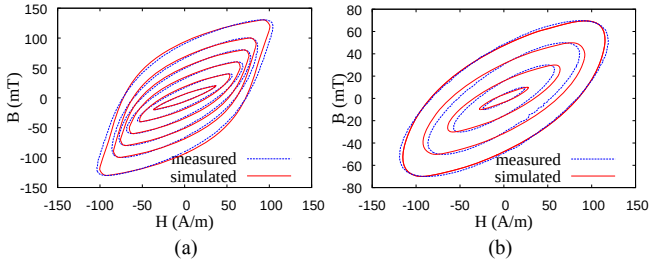

Fig. 10 Simulated BH loops by modified model: (a) at 400 kHz, and (b) at 2 MHz.

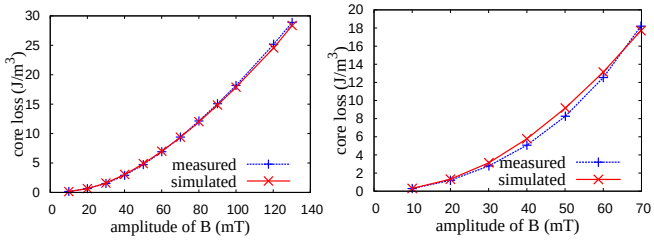

Fig. 11 Core loss per cycle given by modified model: (a) at 400 kHz, and (d) at 2 MHz.

IV. Simulation of DC Biased Properties

The DC bias is supplied from the DC current source and circuitally added to the excitation current without interfering the AC power source. However, the DC bias component of B is not obtained from the secondary winding. This paper assumes that the point (H, B) is located on the normal magnetization curve when B is maximum as is shown in Fig. 12(a), where measured B-H loop is sifted along the B-direction to add an estimated DC component of B.

Fig. 13 shows simulated DC biased minor BH loops, which agree with measured loops. The corresponding core loss and average permeability are shown in Figs. 14 and 15. The average permeability is simply given by $(B_{\max}–B_{\min})$ / $(H(B_{\max})–H(B_{\min}))$ where $B_{\max}$ and $B_{\min}$ are the maximum and

minimum values of B as is shown in Fig. 12(b). The decrease in the average permeability with the increase in the DC bias is evident. The evaluation error of the core loss at 100 mT is 5.1 % and 10.6 % corresponding to Figs. 14(a) and (b). The discrepancy of permeability at 100 mT is 2.5 % and 2.7 % corresponding to Figs. 14(a) and (b). The input-dependent shape function [7] is required for the play model to achieve more accurate representation of the minor BH-loops.

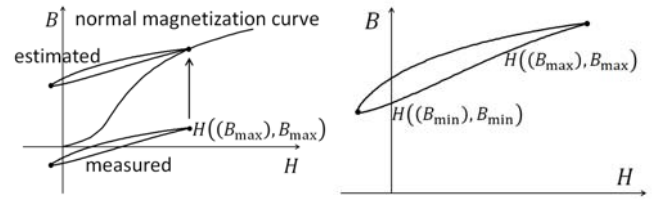

(a) (b)

Fig. 12. Explanations of DC biased minor BH loops: (a) shift along the B-direction, and (b) average permeability.

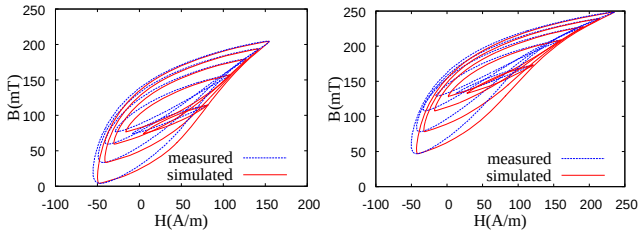

(a) (b)

Fig. 13. DC biased minor BH loops: (a) with DC bias 40 A/m, and (b) with DC bias 80 A/m.

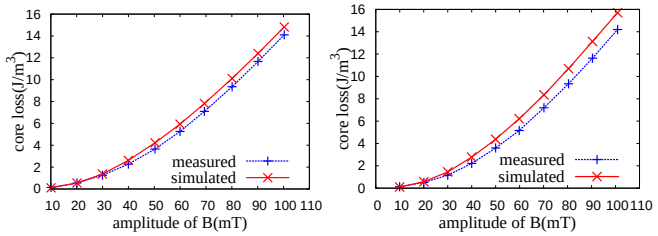

(a) (b)

Fig. 14 Core loss of DC biased condition: (a) with DC bias 40 A/m, and (b) with DC bias 80 A/m.

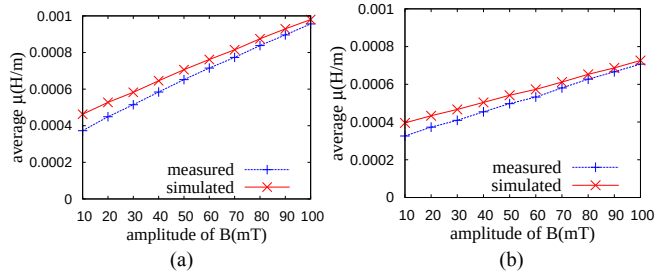

(a) (b)

Fig. 15 Average permeability: (a) with DC bias 40 A/m, and (b) with DC bias 80 A/m.

V. Conclusions

A modeling method is developed to derive an equivalent circuit model for AC and DC ferrite magnetic properties. The combination of the B-input and H-input play models are effectively used for processing hysteretic data. Simulated magnetic properties with or without DC bias agree with the measured properties.

The electric power circuit analysis combined with the proposed model will be reported on in the near future.

Appendix

The H-input play model is written as:

$$B(H) = \sum_{n=1}^{N_p} f_n(p_n(H)) \tag{8}$$

$$p_n(H) = \max(\min(p_n^0, H+\zeta_n), H-\zeta_n) \tag{9}$$

where p_n is the play hysteron operator having width $\zeta_n = nH_S/N_p$, N_p is the number of hysterons, H_S is the saturation magnetic field, and f_n is the shape function for p_n. The Newton-Raphson iteration requires the dB/dH that is obtained from (8) and (9) as:

$$\frac{dB}{dH} = \sum_{n=1}^{N_p} \frac{df_n}{dp_n}\frac{dp_n}{dH} \tag{10}$$

$$\frac{dp_n}{dH} = \begin{cases} 0 & (p_n = p_n^0) \\ 1 & (p_n \neq p_n^0) \end{cases}. \tag{11}$$

The B-input play model is given in a similar way to the H-input model.

Acknowledgment

This work was supported in part by the Adaptable and Seamless Technology Transfer Program through Target-driven R&D, Japan Science and Technology Agency.

References

[1] Richard M. Bozorth, *Ferromagnetism*, IEEE Press, Piscataway 1993.
[2] F. Preisach, "Über die Magnetische Nachwirkung," *Zeitschrift für Physik*, vol. 94, pp. 277-302, 1935.
[3] I.D. Mayergoyz, *Mathematical Models of Hysteresis and their Applications*, Elsevier, New York, 2003.
[4] M.A. Krasnosel'skii and A.V. Pokrovskii, *Systems with Hysteresis*, Springer-Verlag, Berlin Heidelberg, 1989.
[5] M. Brokate, "Some mathematical properties of the Preisach model for hysteresis," *IEEE Trans. Magn.*, vol. 25, pp. 2922–2924, July 1989.
[6] S. Bobbio, G. Miano, C. Serpico, and C. Visone, "Models of magnetic hysteresis based on play and stop hysterons," *IEEE Trans. Magn.*, vol. 33, pp. 4417-4426, Nov. 1997.
[7] T. Matsuo and M. Shimasaki, "An identification method of play model with input-dependent shape function," *IEEE Trans. Magn.*, vol. 41, pp. 3112-3114, Oct. 2005.
[8] T. Matsuo, Y. Terada, and M. Shimasaki, "Stop model with input-dependent shape function and its identification methods," *IEEE Trans. Magn.*, vol. 40, pp. 1776-1783, July 2004.
[9] T. Matsuo, M. Miyamoto, "Dynamic and anisotropic vector hysteresis model based on isotropic vector play model for non-oriented silicon steel sheet," *IEEE Trans. Magn.*, Vol. 48, pp. 215-218, Feb. 2012.
[10] K. Fujiwara, Y. Okamoto, A. Kameari, A. Ahagon, "The Newton-Raphson method accelerated by using a line search −comparison between energy functional and residual minimization," *IEEE Trans.* Magn., vol. 41, pp.1724-1727, May 2005.
[11] K. Kondo, T. Chiba, S. Yamada, "Effect of microstructure on magnetic properties of Ni–Zn ferrites," *J. Magn. Magn. Mater.*, vol. 254–255, pp. 541–543, 2003.